A Compact Magnetically Insulated Line Oscillator with New-Type Beam Dump *

FAN Yu-Wei(樊玉伟)[1,2**], SHU Ting(舒挺)[1], LIU Yong-Gui(刘永贵)[1], ZHONG Hui-Huang(钟辉煌)[1], LI Zhi-Qiang(李志强)[1], WANG Yong(王勇)[1], ZHAO Yan-Song(赵延宋)[1], LUO Ling(罗玲)[1]

[1] *College of Optoelectrical Science and Technology, National University of Defence Technology, Changsha 410073*
[2] *Air Defence Command Academy, Zhengzhou 450052*

(Received 9 July 2004)

We present a compact improved model of the magnetically insulated line oscillator with new-type beam dump and other novel features. In the experiments, high-power microwave of the TM_{01} mode is generated from the device with a frequency range of 1.73–1.78 GHz and a peak power level of above 2 GW, when the diode voltage is taken in the range 520–540 kV, and the diode current is in the range 58–62 kA. This confirms the simulation results.

PACS: 52.59.−f, 52.65.Rr, 52.70.Gw

The magnetically insulated line oscillator (MILO) is a relatively new type of coaxial crossed field microwave device designed specifically to generate microwave power at the gigawatt level. It requires no externally applied magnetic field to insulate the electron flow in the slow-wave structure (SWS). This self-insulating property, inherent in magnetically insulated lines, allows the device to handle an extremely large input beam power (tens of gigawatts) without ensuing electrical breakdown of the anode–cathode gap (AK gap).[1−5]

The investigated device is illustrated in Fig. 1. The configuration is cylindrically symmetric about the z-axis. It consists of a four-cavity SWS, preceded by a one-cavity rf choke section. Both the choke vanes and the SWS vanes are connected to a cast iron outer of the conductor. The last vane of the SWS is also part of the extractor, so it is referred to as the extractor vane. The inner radius of the extractor vane is slightly larger than that of the SWS vanes to provide a good match of the gap electric field to that of the output coaxial transmission line (CTL).[1] The load region is comprised of both the right end and the end surfaces of the cathode, a beam dump disc and the inner-conductor of the output CTL. The mode converter is supported by the two inner conductor-based sets of conducting rods which also serve as the current return path from the beam dump.

The electron beam emission region is confined by placing velvet on the cathode running from the upstream side of the second choke vane to the right end of the cathode and the end surface of the cathode. The velvet is used as the emitting surface and is pasted on the cathode with conducting glue.

The principle of the MILO, using Fig. 1 for reference, is described as follows. A high-voltage pulse is introduced from the left and propagates to the right in Fig. 1. Electrons are emitted from the cathode. The load current generates the dc magnetic field in the SWS section, which prevents electrons emitted on the cathode from reaching the anode. This self-insulating property inhibits electrical breakdown of the AK gap. At the same time, this dc magnetic field plays a key role in the synchronism between the drifting electrons and a certain electromagnetic wave, whose characteristics are determined by the SWS, transferring energy from the electron beam to the electromagnetic wave. The growing electromagnetic wave induces an rf voltage across the extractor gap which produces a TEM wave in the coaxial section around the beam dump.[2] The TEM wave propagates down the section of coaxial waveguide and is transformed into the TM_{01} mode by a mode converter, and is then launched into a circular waveguide, where it propagates in the TM_{01} mode.

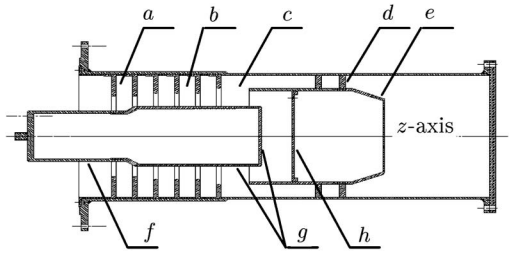


Fig. 1. Configuration of the investigated MILO: (a) rf choke cavity, (b) slow-wave structure, (c) extractor gap, (d) rod, (e) mode converter, (f) cathode, (g) velvet, (h) beam dump disc.

For the sake of more efficient operation and more compact structure, a new-type beam dump and other three novel features have been introduced into this improved MILO.

As illustrated in Fig. 2, a beam dump disc is added into the beam dump, with the consideration of the layout of the beam dump in the taped MILO.[4] The new-

* Supported by the National High Technology Program of China under Grant No 2002AA834020.
** Email: 9108212@sohu.com
©2005 Chinese Physical Society and IOP Publishing Ltd

type beam dump has two advantages. First, the axial distance from the cathode to the beam dump disc can be adjusted continuously through axial movement of the beam dump disc. The axial distance affects the load current, and hence the dc magnetic field in the SWS. If the axial distance is too large, the insulating of this dc magnetic field will be insufficient and the electrons in the SWS would just flow out to the vanes, initiating an arc. If the axial distance is not large enough, the insulating will be too strong, pulling the electron flow away from the inner radius of the SWS. At the same time, changing of the dc magnetic field will affect the synchronism between the electrons and the wave. All these will weaken the energy coupling into the electromagnetic wave. Through adjusting the axial distance, the optimal operating state can be found to increase the power conversion efficiency and thus the radiation power. Simulations and experiments have consistently shown that an improper axial distance from the cathode to the beam dump disc seriously degrades the MILO performance. For example, experiments show that only a 5-mm shift of the axial distance from its optimal value results in an over 40% drop in the output power. In the conventional MILO,[1−3,5] however, it is difficult to adjust the dc magnetic field because no part of it can be moved easily. Therefore, this improved device is able to operate at the optimal state more easily than the conventional MILO, which leads to the more efficient generation of microwaves. Second, the device is more compact than the conventional MILO. As mentioned above, in the compact MILO, the electrons of the load current are emitted from both the side and the end surface of the cathode extended into the beam dump region. According to simulation, the end surface of the cathode provides more than one half of the total electrons. However, in the conventional MILO (see Fig. 2 in Ref. [2]), the electrons of the load current are emitted only from the side of the cathode extended into the beam dump region. Therefore, in order to generate the same load current, the length of the cathode extended into the beam dump region will be reduced in the case of the compact MILO. Consequently, the device is expected to be shorter than the conventional MILO.

Apart from the new-type beam dump mentioned above, the following three approaches of improvement are also employed. Firstly, a one-cavity rf choke section is introduced into the compact MILO. The rf choke section has a different passband from the SWS and serves as an in-phase reflector of the rf power leaking toward the pulsed power input.[5] Through numerical simulation, the reflectivity of the leaking rf power is optimized to attain 99.4%. This improvement further reduces the length of the device as compared with the conventional MILO. Secondly, the carefully designed impedance discontinuity between the choke-vane section and the SWS-vane section can benefit to the operation of the MILO. On the one hand, the large impedance in the choke-vane section results in a lower electric field at this section, avoiding electric breakdown. On the other hand, the small impedance in the SWS-vane section results in a higher spoke current than the one when the sections of both the choke-vanes and the SWS-vanes have the same impedance. A higher spoke current has more electrons near the surface of the SWS, the desired interaction region where the rf fields are the strongest, than does a lower spoke current. This results in a substantial increase in power conversion efficiency.[3] Thirdly, a new-type mode converter is employed in the compact MILO. The numerical simulation shows that this kind of mode converter is more efficient to transform the TEM mode into the TM_{01} mode than that in the conventional MILO. Through numerical optimization, the mode converter designed can achieve such a high power conversion efficiency as over 98%, with the consideration of the affecting of the supporting conducting rods.

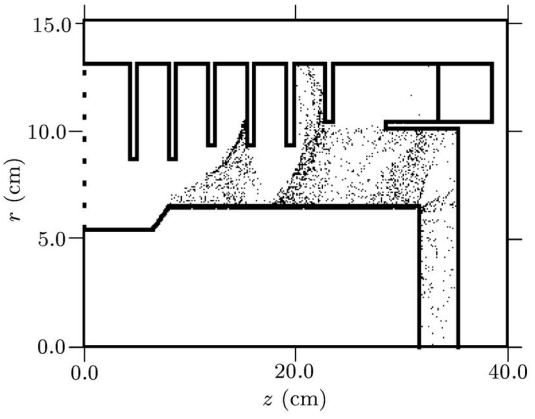


Fig. 2. Distribution of the particles.

To simulate and optimize the compact MILO operation, a fully electromagnetic particle-in-cell code[6−8] is used. The simulation model for the compact MILO is shown in Fig. 2. It should be noted that only a part of the compact MILO involved in beam-wave interaction is included in the model, with the rest designed through numerical simulation. The total length of the designed device is 70 cm, and the diameter 26 cm, much smaller in overall size than the conventional-MILOs.[1−3,5]

The electron distribution in Fig. 2 illustrates the quasi π-mode operation of the device. In the π-mode, the electric fields in adjacent cavities are 180 deg out of phase, which causes the electrons to be attracted to alternating cavities and repelled elsewhere.[2] When a device is operated in the π-mode, which is the highest Q (quality factor) spatial harmonic associated with the SWS, and also, the field distribution associated

with the π-mode produces the strongest coupling to the electron flow.[2]

Figures 3 and 4 are also the results from particle-in-cell simulation of the compact MILO. Figure 3 is the rf output power versus time, and the averaged rf output power is 2.3 GW. Figure 4 is the rf output power spectrum, with a central frequency of 1.75 GHz. In this case, the applied voltage and current is 540 kV and 49 kA respectively, and the corresponding power conversion efficiency is calculated to be 8.7%.

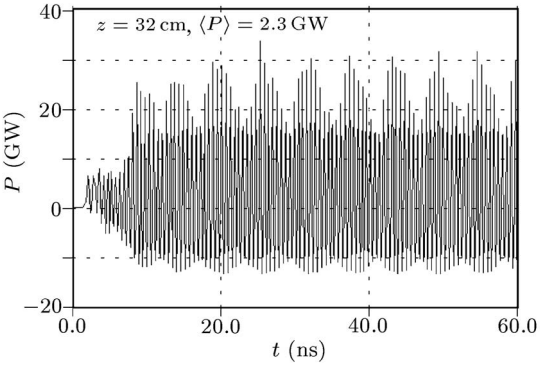


Fig. 3. The rf output power versus time.

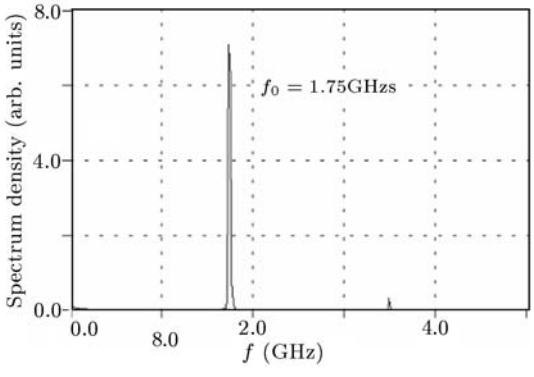


Fig. 4. The rf output power spectrum.

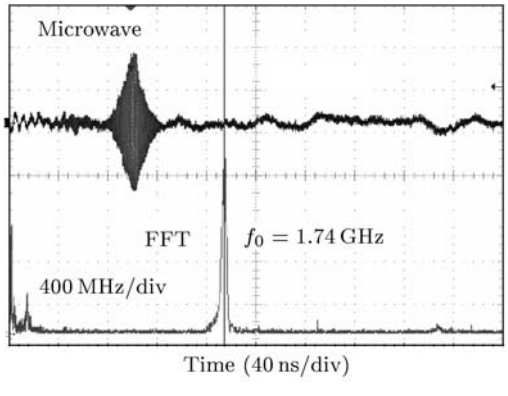


Fig. 5. The radiated microwave and its spectrum.

The experiments are carried out on the device, which has been fabricated in accordance with the optimized configuration. The compact MILO is driven by a self-built 600 kV, 8 Ω, 100 ns pulser: SPARK-01. The radiated microwave is detected with the far-field measurement method.[9] The generated microwave radiation is received simultaneously by two horns located in the far-field zones, which are used for the measurement of the radiation frequency, and pattern, and hence of the radiation power.

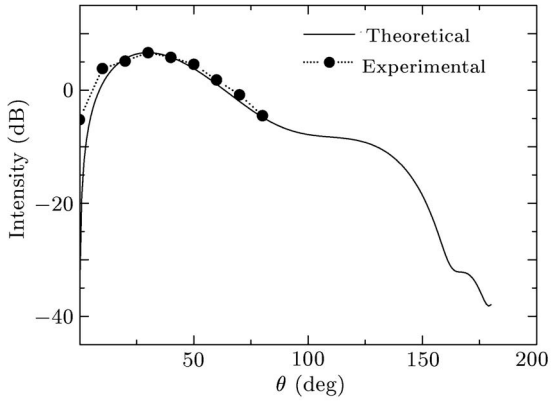


Fig. 6. The measured radiation pattern.

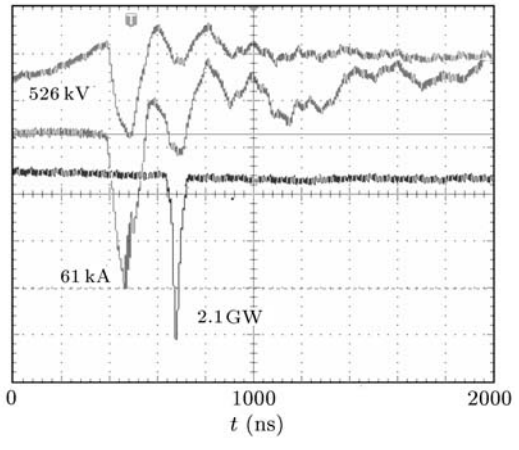


Fig. 7. The measured waveforms.

Figure 5 shows the signal from an oscilloscope of TDS 7154, which measures the radiation frequency by fast Fourier transform (FFT) of the received time-dependent waveform. The main radiation frequency is measured to be 1.73–1.78 GHz. The measured radiation pattern shown in Fig. 6 is obtained when the microwaves radiate from the open end of the circular waveguide. The obtained radiation pattern (TM_{01} mode) agrees well with that obtained theoretically under the same conditions. In Fig. 6, the minor non-zero value on the axis (at $\theta = 0$) indicates the co-radiation of the TE_{11} mode, of which the power is less than 1% of the one in the TM_{01} mode. Figure 7 shows the waveforms of the diode voltage, the diode current and

the radiated microwave. The radiation peak power from the compact MILO is calculated to be 2.1 GW based on the obtained radiation frequency and mode, as well as the measured power density. In this case, the diode voltage is 526 kV, and the diode current 61 kA. The duration of the effective voltage (above the threshold voltage 450 kV) is 50 ns, and the duration of the radiated microwave 32 ns (FWHM).

In conclusion, a compact MILO has been presented with new-type beam dump and other three novel features. Its configuration and operation condition are optimized through PIC and numerical simulation. This modified configuration of the device has been examined by experiment extensively. The measured microwave frequency ranges from 1.73 GHz to 1.78 GHz, with a peak power level of above 2 GW. The experimental results confirm the ones predicted by simulation, with the diode voltage ranging in 520–540 kV, and the beam current in 58–62 kA.

References

[1] Lemke R W, Calico S E and Clark M C 1997 *IEEE Trans. Plasma Sci.* **25** 364
[2] Calico S E, Clark M C, Lemke R W and Scott M C 1995 *Proc. SPIE* **2557** 50
[3] Haworth M D, Luginsland J W and Lemke R W 2000 *IEEE Trans. Plasma Sci.* **28** 511
[4] Eastwood J W, Hawkins K C and Hook M P 1998 *IEEE Trans. Plasma Sci.* **26** 698
[5] Haworth M, Allen K, Baca G and Benford J 1997 *Proc. SPIE* **3158** 28
[6] Shu T, Wang Y, Qian B L and Tan Q M 2002 *Chin. Phys. Lett.* **19** 1646
[7] Zhang J, Zhong H H, Shu T and Yang J H 2003 *Chin. Phys. Lett.* **20** 2265
[8] Yang J H, Zhang Y Z, Zhang J D, Shu T and Li C L 2003 *Chin. Phys. Lett.* **20** 96
[9] Shu T, Wang Y, Li J J, Xi F 2003 *High Power Laser Part. Beams* **15** 485 (in Chinese)